ELSEVIER

Materials Science and Engineering A xxx (2007) xxx–xxx

MATERIALS SCIENCE & ENGINEERING A

www.elsevier.com/locate/msea

As-cast mechanical properties of vanadium/niobium microalloyed steels

Hamidreza Najafi [a,*], Jafar Rassizadehghani [a,1], Siroos Asgari [b,1]

[a] *School of Metallurgy and Materials Engineering, University College of Engineering, University of Tehran, P.O. Box 14395-731, Tehran, Iran*
[b] *Department of Materials Science and Engineering, Sharif University of Technology, P.O. Box 11365-9466, Tehran, Iran*

Received 17 April 2007; received in revised form 16 August 2007; accepted 27 August 2007

Abstract

Tensile and room temperature Charpy V-notch impact tests along with microstructural studies were used to evaluate the variations in the as-cast mechanical properties of low-carbon steels with and without vanadium and niobium. Tensile test results indicate that good combinations of strength and ductility can be achieved by microalloying additions. While the yield strength and UTS increase up to respectively 370–380 and 540–580 MPa in the microalloyed heats, their total elongation range from 20 to 25%. TEM studies revealed that random and interphase fine-scale microalloy precipitates play a major role in the strengthening of the microalloyed heats. On the other hand, microalloying additions significantly decreased the impact energy and led to the dominance of cleavage facets on the fracture surfaces. It seems that heterogeneous nucleation of microalloy carbonitrides on dislocations along with coarse ferrite grains and pearlite colonies trigger the brittle fracture in the microalloyed heats.

Keywords: Cast steel; Microalloyed steel; Niobium; Vanadium

1. Introduction

Although wrought grades of microalloyed steels have been available for years, demands for producing low-cost, higher strength steel castings with good toughness and weldability have encouraged some researchers to focus on cast grades of these steels. Microalloyed cast steels are basically low to medium carbon steels with manganese levels in the 1.2–2 wt% range, and additions of conventional microalloying elements such as titanium, niobium, and vanadium [1,2]. Some grades of microalloyed cast steels, especially French grades, are alloyed with nickel [3]. These steels exhibit a combination of high strength with good toughness and weldability. Nowadays, microalloyed cast steels have found many applications in the manufacturing of industrial parts such as offshore platform nodes, centrifugal cast pipes, machinery supports, nuclear reactor support frames, natural gas compressor housing, ingot moulds and buckets which were all produced by expensive manufacturing processes before [2,4].

Since most of these parts have to be heat treated before use, the effects of different heat treatment variables have been the subject of many investigations [3–7]. The heat treatment of these steels has been generally performed in three stages: homogenization, austenitization followed by quenching or air cooling, and tempering at subcritical temperatures. It has also been reported that special intercritical heat treatments can be used to improve the toughness of these materials. Basically, the ultimate goal of these heat treatments is to benefit from fine ferrite grains by controlling austenite grain growth and precipitation hardening. Hence, the microalloying elements niobium and vanadium are added to microalloyed cast steels primarily to provide grain refinement and response to aging. Niobium, often at levels of less than 0.05%, effectively prevents undesirable grain growth and can also contribute to precipitation strengthening. Vanadium, in particular, at levels of less than 0.1% forms strengthening carbonitride precipitates [8–12].

In contrast to the heat-treated grades, mechanical and microstructural properties of as-cast microalloyed steels have not been investigated yet. Therefore, it seems valuable to study the mechanical properties of the cast microalloyed steels in the as-cast condition in order to examine the possibility of achieving good combinations of properties and producing some industrial parts with these inexpensive steels.

The objective of this study was to assess the influence of vanadium and niobium as microalloying additions on the strength and impact toughness of a low-carbon steel in the as-cast condition.

* Corresponding author. Tel.: +98 21 8208 4066; fax: +98 21 8800 6076.
E-mail addresses: hnajafi@ut.ac.ir (H. Najafi), jghani@ut.ac.ir (J. Rassizadehghani), sasgari@sharif.edu (S. Asgari).
[1] Tel.: +98 21 8208 4066; fax: +98 21 8800 6076.

0921-5093/$ – see front matter © 2007 Elsevier B.V. All rights reserved.
doi:10.1016/j.msea.2007.08.057

Table 1
Chemical compositions of the alloys studied (wt%)

Designation	C	Mn	Si	P	S	Al	V	Nb
B	0.15	1.56	0.35	0.01	0.015	0.03	–	–
V	0.15	1.41	0.31	0.01	0.015	0.02	0.09	–
Nb	0.14	1.50	0.33	0.008	0.010	0.03	–	0.04

2. Experimental procedure

2.1. Materials

A 100 kg capacity, 125 kW, 3 kHz basic lined induction furnace was used for melting. After complete melting of base material, graphite and ferromanganese were added to the melts to adjust carbon and manganese contents. The heats were appropriately deoxidized with ferrosilicon and Al shot. Microalloying elements were added to the melts in the form of ferrovanadium and ferroniobium. The base composition for all heats was selected to be about 0.15 wt% carbon and 1.5 wt% manganese. Vanadium and niobium levels in microalloyed heats were selected to be respectively about 0.1 and 0.04. Furthermore, sulfur plus phosphorous levels ranged from 0.02 to 0.035% for all heats. Table 1 shows the chemical compositions of the heats (B stands for the base composition). All heats were poured directly from the furnace into the moulds at 1590 °C. The test materials were produced in the form of 3-in. Y-blocks using sand moulds.

2.2. Microstructural characterization

Metallographic samples were prepared using standard polishing techniques and were then etched with 2% Nital. An Omnimet image analyzer was used to measure the area fraction of pearlite. Since ferrite grains were not equiaxed in the as-cast microstructures, the ferrite mean free path was used to characterize the fineness of ferrite phase by using following equation [13]:

$$\lambda = \frac{V_{V\alpha}}{N_L}$$

where $V_{V\alpha}$ is the volume fraction of ferrite and N_L is the number of ferrite intercepted per unit length. Twenty measurements were recorded for every microstructure and the average was taken as the area fraction of pearlite and ferrite mean free path.

Etched samples were studied in a CamScan SEM equipped with an Oxford instruments EDS analyzer in order to observe the microstructures more closely. In addition, fractographic examinations of the impact specimens were carried out to allow a better understanding of the micromechanisms of fracture in different alloys.

For TEM studies, slices of about 400 μm in thickness were cut using an electro-discharge machine (EDM). These samples were subsequently ground to a thickness of 100 μm. Discs of about 3 mm in diameter were punched from the thinned wafers and TEM foils were prepared by electropolishing these discs in a Fishione twin jet unit. A solution of 10% perchloric acid in acetic acid electrolyte was used for electropolishing. The foils were examined by a Philips 400T scanning transmission electron microscope operating at 120 kV.

2.3. Mechanical properties

To evaluate mechanical properties, tensile, microhardness, and standard room temperature Charpy V-notch (CVN) tests were conducted. Three tensile specimens prepared according to ASTM-E8 from different parts of each block were tested in an MTS tensile testing machine of 150 kN capacity at a crosshead speed of 1 mm min^{-1}. Three Charpy impact specimens were also prepared from different parts of each block according to ASTM-E23 and tested at room temperature. Vickers microhardness measurements were taken from individual ferrite grains using a load of 5 g. Measurements from 100 grains on each sample were used to calculate the mean value of hardness.

3. Results and discussion

3.1. Microstructural characterization

Optical microscopy studies revealed that the addition of microalloying elements did not considerably change the main microstructural features due to the fact that all microstructures consisted of coarse ferrite grains and pearlite. Representative optical micrographs of the base and microalloyed heats are presented in Fig. 1.

Image analysis and linear intercept method were used to measure pearlite content and ferrite mean free path in order to study the microstructural changes due to the microalloying additions. The results summarized in Table 2 show that the pearlite content in the Nb-bearing heat has increased from 26 to 29%. In other words, the presence of niobium increases pearlite content while vanadium addition does not change it. The observed increase in pearlite content of the Nb-bearing alloy can be related to the behavior of free Nb atoms in austenite which has been recognized as "non-equilibrium segregation" or "quenched-induced segregation" [14,15]. Previous investigations have suggested that Nb atoms segregate to certain microstructural regions such

Table 2
Pearlite content and ferrite mean free path in different alloys

Designation	Ferrite mean free path (μm) ±95% CL[a]	Pearlite content (%) ±95% CL
B	59 ± 2	26 ± 1
V	61 ± 4	26 ± 1
Nb	46 ± 4	29 ± 2

[a] 95% confidence limit.

Please cite this article in press as: H. Najafi, et al., Mater. Sci. Eng. A (2007), doi:10.1016/j.msea.2007.08.057

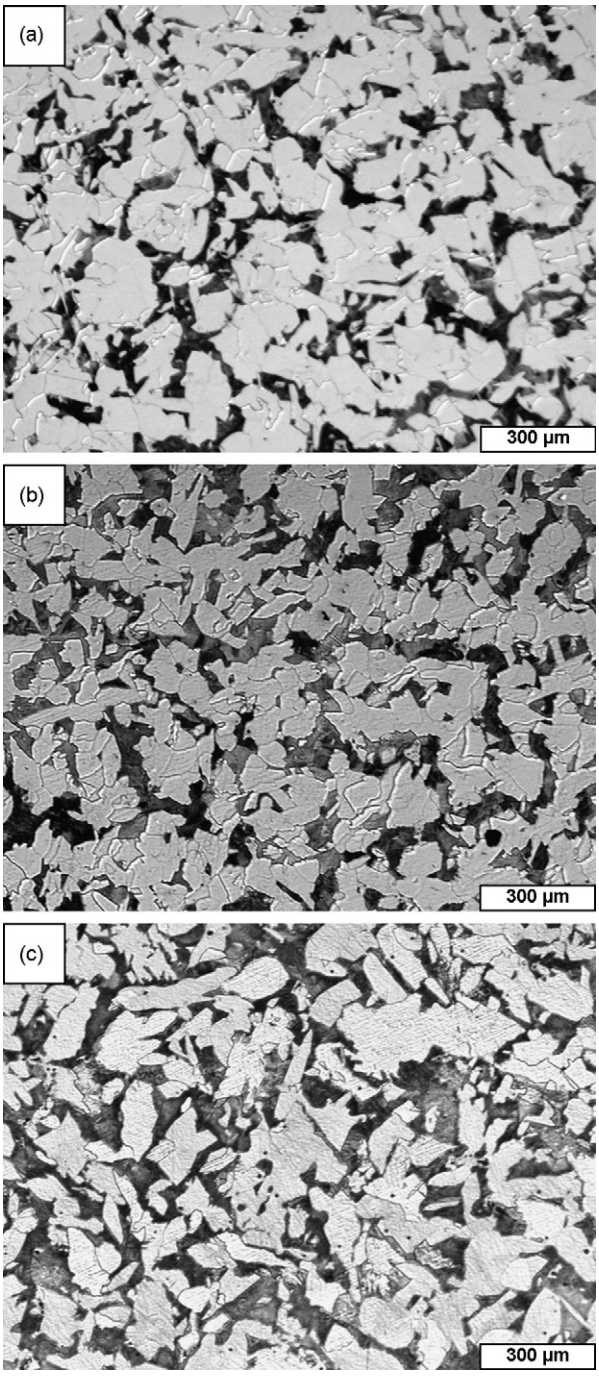

Fig. 1. Optical microstructure of (a) alloy B, (b) alloy V, and (c) alloy Nb.

as γ/α and γ/γ boundaries [14–16]. As a result, γ → α transformation is retarded and Ar_3 decreases due to the solute drag effect [17,18].

The results of ferrite mean free path measurements shown in Table 2 indicate that while addition of vanadium does not considerably change the ferrite mean free path, the presence of Nb decreases it. This behavior can be justified by taking into account the effect of Nb on γ → α transformation indicated in the aforementioned paragraph. In other words, the decrease in Ar_3 can be the reason for the observed reduction in ferrite grain size.

3.2. Fine-scale precipitates

TEM studies carried out on the microalloyed heats in order to study fine-scale precipitates having been formed in the ferritic matrix, revealed carbonitrides being 10 nm or less in size. Based on the observations, three different states including random precipitation, interphase precipitation, and heterogeneous precipitation on the dislocations could be identified. Since the precipitation behavior was similar in these alloys, the discussion will be restricted to alloy V in this section.

Fig. 2a shows a bright field TEM micrograph of fine precipitates distributed randomly and Fig. 2b shows the corresponding composite SAD pattern. The diffraction pattern analysis showed the presence of a B1 (NaCl) type FCC unit cell of vanadium carbonitride. Lattice parameter measurement made from the SAD pattern suggested that the precipitates were carbon rich since the calculated value was about 4.10 Å which is very close to the predicted value of 4.15 Å for vanadium carbide. Furthermore, the orientation relationship between ferrite and vanadium carbide was a cube–cube $[0\,0\,1]_{\alpha}//[0\,0\,1]_{VC}$ Baker–Nutting relationship.

Fig. 3a depicts parallel sheets containing fine particles formed repeatedly with regular spacing. The SAD pattern obtained from one of the particles (Fig. 3b) indicated that it had an NaCl-type structure with B–N orientation relationship with the ferritic matrix. Many TEM studies on microalloyed steels have demonstrated the formation of interphase precipitation of carbonitrides in the form of sheets which are parallel to the γ/α interface. In addition, they have proved that the precipitates in the sheets have B–N orientation relationship with ferrite [19–24]. Hence, it can be concluded that the sheets depicted in Fig. 4a are in fact clusters of fine interphase vanadium carbide precipitates. Moreover, being perpendicular to the sheets, the orientation of transformation front can be inferred from this micrograph.

Fig. 4a illustrates another precipitation state in which carbonitride particles are located on dislocations. Recent studies on microalloy precipitates formed in ferrite grains, have shown that they prefer to nucleate heterogeneously on dislocations in order to reduce the strain field which stems from lattice parameter difference between the precipitates and ferrite [25–29].

3.3. Mechanical properties

The results obtained from tensile and CVN tests are reported in Table 3. Properties reported in this table are the average properties of different testing specimens from different positions within casting sections. According to these results, the presence of microalloying elements significantly increased the yield strength and UTS, at the expense of some reduction in elongation, but considerable decrease in impact toughness. Microalloying elements increased yield strength and UTS up to 100 MPa. However, it seems that niobium is more efficient than vanadium in enhancing the strength due to the fact that yield strength and UTS of alloy Nb containing 0.04% niobium are approximately equal to alloy V containing 0.1% vanadium.

The observed increase in the yield strength and UTS of microalloyed heats can be attributed to several factors such as variations in pearlite content, ferrite mean free path, and

Please cite this article in press as: H. Najafi, et al., Mater. Sci. Eng. A (2007), doi:10.1016/j.msea.2007.08.057

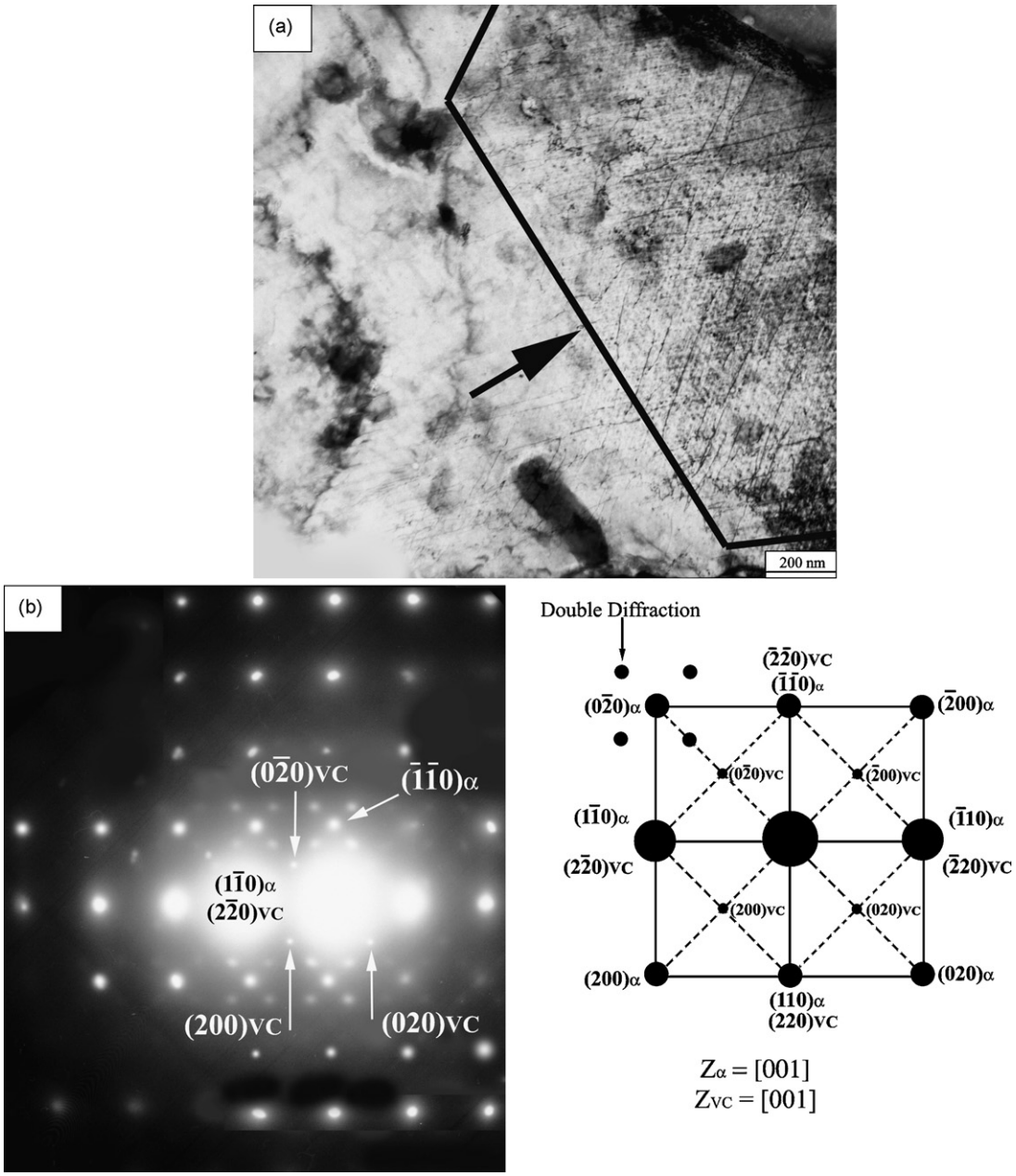

Fig. 2. (a) Bright field TEM micrograph showing a region (indicated by arrow) in which fine vanadium carbides have precipitated randomly and (b) SAD pattern for the image (a) depicting zone $[0\,0\,1]_{\alpha}$ of ferrite is parallel to $[0\,0\,1]_{VC}$ zone of vanadium carbide with ordered B1 (NaCl) type unit cell.

formation of fine-scale carbonitride precipitates. Quantitative metallography results, however, imply that the first and second factors do not play a major role in enhancing the strength of microalloyed heats due to the fact that the strength of alloy V, which has almost the same pearlite content and ferrite mean free path as alloy B, is more than the base heat. Moreover, the observed differences in the ferrite mean free path and pearlite content between alloys B and Nb are not so considerable to pro-

Table 3
Mechanical properties of the alloys studied

Designation	Yield (MPa) ± S.D.[a]	UTS (MPa) ± S.D.	Elongation (%) ± S.D.	Microhardness (HVN) ± S.D.	Room temperature impact energy (J) ± S.D.
B	272 ± 8	470 ± 6	30 ± 1	117 ± 8	79 ± 6
V	378 ± 8	579 ± 8	23 ± 1	156 ± 5	20 ± 5
Nb	374 ± 4	542 ± 6	20 ± 2	150 ± 6	9 ± 3

[a] Standard deviation.

Please cite this article in press as: H. Najafi, et al., Mater. Sci. Eng. A (2007), doi:10.1016/j.msea.2007.08.057

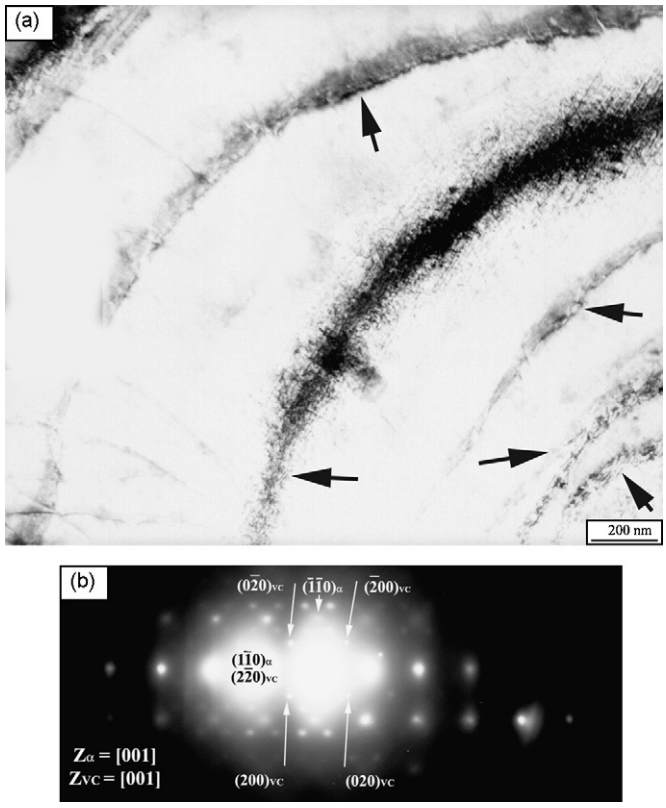

Fig. 3. (a) Bright field TEM micrograph showing parallel sheets (indicated by arrows) containing fine vanadium carbide precipitates and (b) SAD pattern for the image (a) depicting zone $[0\,0\,1]_{\alpha}$ of ferrite is parallel to $[0\,0\,1]_{VC}$ zone of vanadium carbide with ordered B1 (NaCl) type unit cell.

duce such a significant strengthening. Therefore, the observed increase in the microalloyed heats can be related to the fine-scale carbonitrides formation.

Carbonitrides precipitation has been the subject of many investigations having studied different aspects of the precipitates and their effects on the mechanical properties. Although most of these investigations have been restricted to the wrought grades or heat-treated cast steels, their findings can be applied to the present research. Based on these studies, effective carbonitrides in strengthening are those formed finely with adequate distribution especially in ferrite grains. Therefore, microalloy carbonitrides precipitating on the advancing γ/α interface, i.e. interphase precipitation, and from supersaturated ferritic matrix, i.e. random precipitation, play a major role in precipitation hardening in microalloyed steels [19–24]. As a result, the increase observed in the strength of the microalloyed heats can be attributed to the precipitation of fine-scale carbonitrides in the form of interphase (Fig. 3a) and random (Fig. 2a) precipitates.

Microhardness measurements of individual ferrite grains were conducted to compare the significance of precipitation hardening in alloys V and Nb. The results shown in Table 3 indicate that the mean values of ferrite microhardness have increased in alloys V and Nb. This increase can essentially be brought about by precipitation hardening rather than solid solution hardening since provided there are free microalloying atoms after cabonitrides formation, the solid solution hardening caused by them is negligible due to their very low concentration. The same microhardness values of alloys V and Nb implies that niobium despite its lower content is more potent than vanadium in pre-

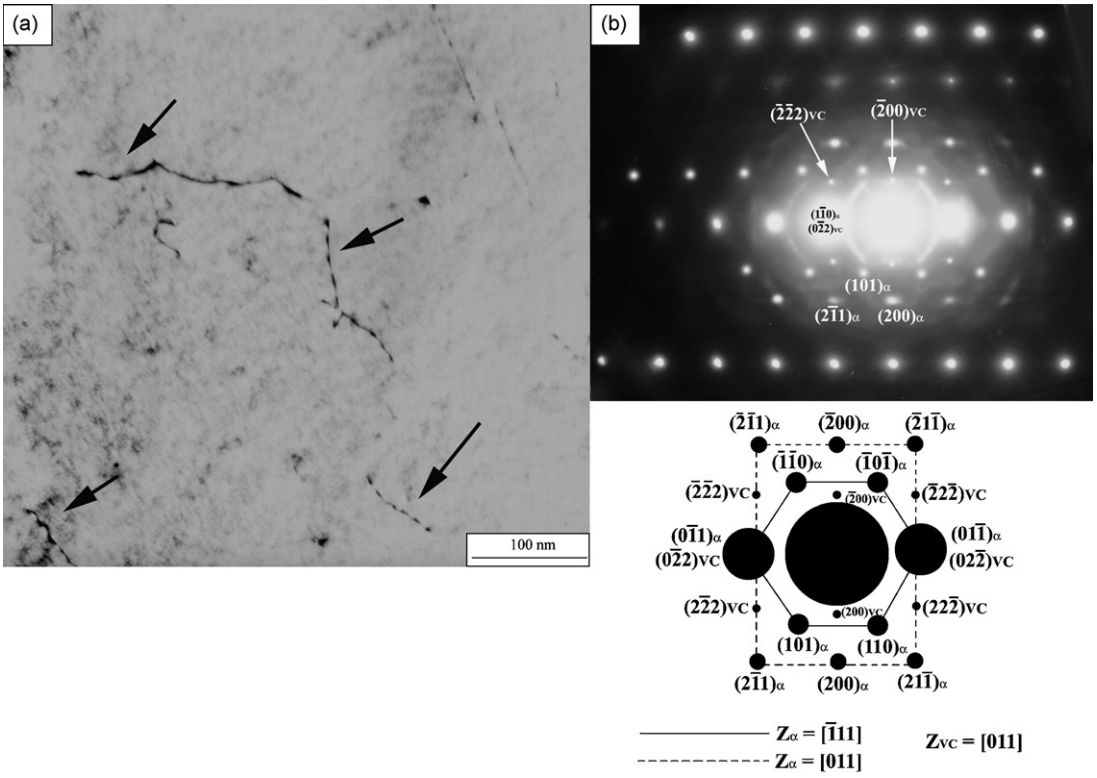

Fig. 4. (a) Bright field TEM micrograph showing precipitation of fine carbides on dislocations (indicated by arrows) and (b) SAD pattern for the image (a) depicting two zones $[0\,1\,1]_{\alpha}$ and $[\bar{1}\,1\,1]_{\alpha}$ of ferrite are parallel to $[0\,1\,1]_{VC}$ zone of vanadium carbide with ordered B1 (NaCl) type unit cell.

Please cite this article in press as: H. Najafi, et al., Mater. Sci. Eng. A (2007), doi:10.1016/j.msea.2007.08.057

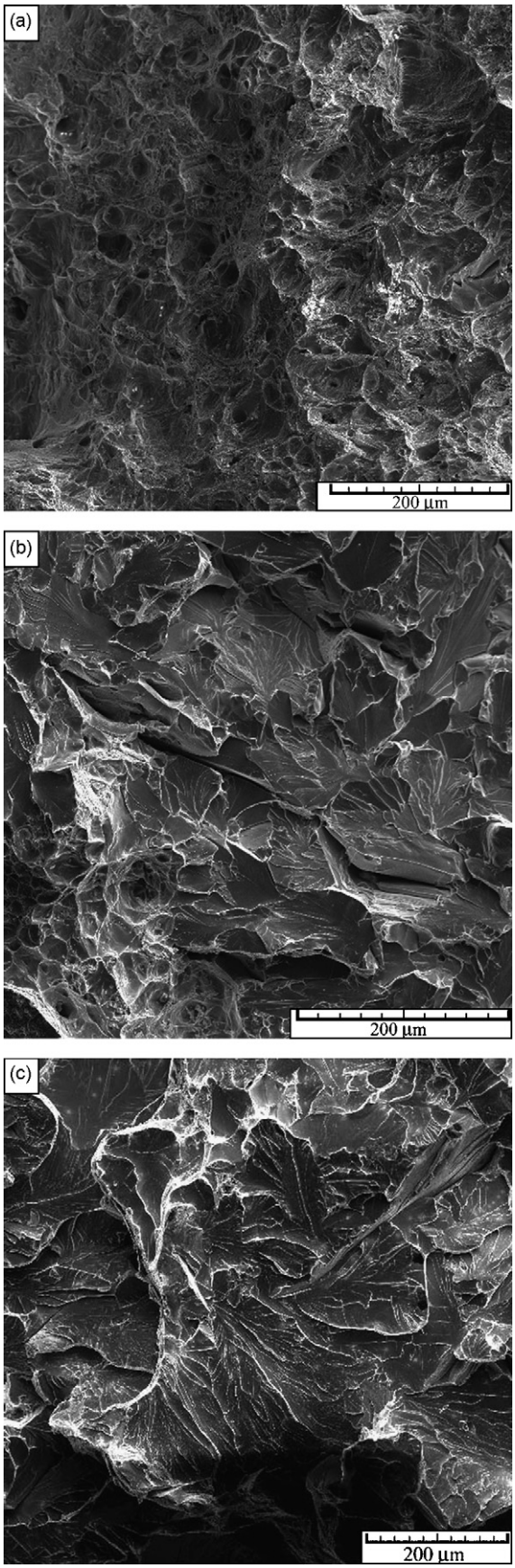

Fig. 5. Scanning electron fractograph showing (a) ductile failure in the base heat and (b and c) brittle failure in alloys V and N.

cipitation hardening. Many investigations have pointed out that niobium cabonitride is less soluble than vanadium cabonitride in austenite and ferrite. Therefore, at a certain temperature, the driving force for niobium carbonitride precipitation is considerably larger than vanadium carbonitride. Accordingly, niobium can contribute more efficiently than vanadium to dispersion hardening.

The results in Table 3 show that elongation and Charpy impact energy values have decreased due to the presence of microalloying elements. While the decrease in elongation values can be attributed to the increase in strength levels, the rationalization of the decrease in Charpy impact energy values is more complicated. Fractography of impact specimens confirmed the drastic decrease in impact energy of microalloyed samples due to the fact that the fracture surfaces of microalloyed samples were dominated by cleavage facets while the fracture surface of alloy B was dominated by microvoid coalescence (Fig. 5).

The micromechanisms by which ductile failure occurs in steels have been studied extensively. Based on these studies, the decohering of MnS particles plays a major role in the nucle-

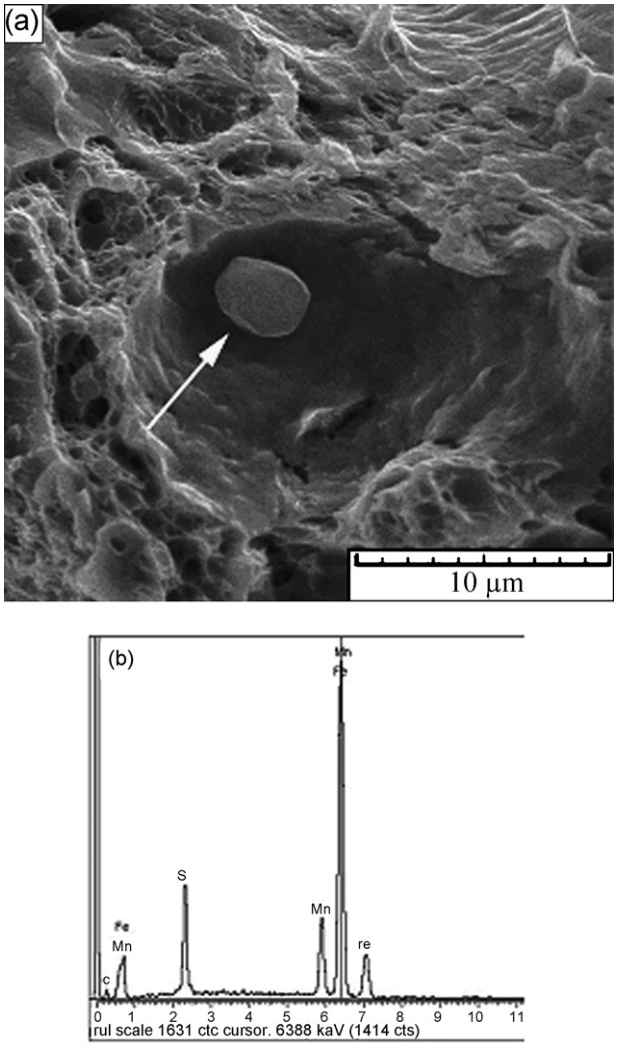

Fig. 6. Scanning electron fractograph of alloy B showing (a) an MnS inclusion in a dimple and (b) X-ray analysis of the particle.

Please cite this article in press as: H. Najafi, et al., Mater. Sci. Eng. A (2007), doi:10.1016/j.msea.2007.08.057

ation of dimples [30]. Fig. 6 shows an example of MnS inclusion acting as a dimple nucleation site.

Since previous studies on Ti-bearing microalloyed ferrittic–pearlitic steels have concluded that the formation of coarse brittle particles such as TiN can be responsible for the brittleness of these alloys [31–35], many inspections were conducted by SEM on the fracture surfaces of the microalloyed heats. However, no coarse particle or inclusion could be identified as cleavage initiators. Hence, it seems that other mechanisms are responsible for cleavage fracture of alloys V and Nb. Fig. 5a shows that fine-scale precipitates prefer to nucleate heterogeneously on dislocations. Recent studies on microalloy precipitates forming in ferrite grains have shown that they prefer to nucleate heterogeneously on dislocations in order to reduce the strain field which stems from lattice parameter difference between the precipitates and ferrite [25–29]. Accordingly, carbonitrides can lock dislocations leading to reduction in their mobility and make microalloyed samples vulnerable to instant loading. On the other hand, coarse ferrite grains provide favorable circumstances for crack propagation by decreasing the number of grains encountered during crack propagation. In other words, although the heterogeneous precipitation is the main reason for the deterioration in impact toughness, coarse ferrite grains also contribute to the embrittlement by facilitating crack propagation.

4. Conclusions

1. Tensile test results indicate that good combinations of strength and ductility can be achieved by microalloying additions. While the yield strength and UTS increase up to 100 MPa, the total elongation is reduced by 10% in the microalloyed heats.
2. TEM studies revealed three different microalloy precipitation states including random precipitation, interphase precipitation, and heterogeneous precipitation on the dislocations in the microalloyed heats.
3. Microhardness measurements of ferrite grains along with TEM studies confirm that the enhancement of strength in the microalloyed heats stems mainly from fine carbonitrides precipitating in the ferrite grains.
4. The equal microhardness values of alloys V and Nb imply that niobium despite its lower content is more potent than vanadium in precipitation hardening. This behavior can be related to larger driving force for niobium carbonitride precipitation.
5. Addition of vanadium to the base composition does not have considerable effect on pearlite content and ferrite grains while addition of niobium refines the ferrite grains and increases the pearlite content. Therefore, it can be concluded that the presence of niobium lowers the critical temperature of austenite to ferrite transformation (Ar_3).
6. Examination of fracture surfaces shows that while the microalloyed heats failed completely by transgranular cleavage, the base sample failed by transgranular ductile failure. SEM observations revealed no distinct microstructural feature as cleavage initiator. However, it is speculated that heterogeneous nucleation of microalloy carbonitrides on dislocations in ferrite along with coarse ferrite grains and pearlite colonies have triggered the brittle fracture in the microalloyed heats.

References

[1] C. Lebeau, AFS Trans. 92 (1984) 645–654.
[2] R.C. Voigt, J.M. Svoboda, Proceedings of 8th International Conference on Offshore Mechanics and Arctic Engineering, vol. 3, ASME, The Hague, Netherlands, March 1989, pp. 353–359.
[3] R.C. Voigt, M. Blair, J. Rassizadehghani, Proceedings of International Conference on 1990 Pressure Vessels and Piping, vol. 201, ASME, Nashville, TN, USA, June 1990, pp. 147–154.
[4] D.L. Albright, S. Bechet, K. Rohrig, Proceedings of International Conference on Technology and applications of HSLA steels, ASM, Philadelphia, PA, USA, 1984, pp. 1137–1153.
[5] R.C. Voigt, J. Rassizadehghani, AFS Trans. 103 (1995) 791–802.
[6] J. Rassizadehghani, R.C. Voigt, Properties and processing of high strength low alloy (HSLA) cast steels, Report 107, Steel Founders' Society of America, USA, 1994.
[7] B.D. Jana, A.K. Chakrabarti, K.K. Ray, Mater. Sci. Technol. 19 (2003) 80–86.
[8] S.N. Prasad, D.S. Sarma, Mater. Sci. Eng. A 399 (2005) 161–172.
[9] S. Shanmugam, M. Tanniru, R.D.K. Misra, D. Panda, S. Jansto, Mater. Sci. Technol. 21 (2005) 165–177.
[10] S. Shanmugam, M. Tanniru, R.D.K. Misra, D. Panda, S. Jansto, Mater. Sci. Technol. 21 (2005) 883–892.
[11] M.I. Vegan, S.F. Medina, A. Quispe, M. Gomez, P.P. Gomez, Mater. Sci. Eng. A 423 (2006) 253–261.
[12] H.J. Kestenbach, S.S. Campos, E.V. Morales, Mater. Sci. Technol. 22 (2006) 615–626.
[13] G.F. Vander Voort, Metallography Principles and Practice, McGraw-Hill, New York, 1984.
[14] W.J. Liu, Metall. Mater. Trans. A 26A (1995) 1641–1657.
[15] M. Jahazi, J.J. Jonas, Mater. Sci. Eng. A 335 (2002) 49–61.
[16] E.J. Palmiere, C.I. Garcia, A.J. DeArdo, Metall. Mater. Trans. A 27A (1996) 951–960.
[17] P.A. Manohar, T. Chandra, C.R. Killmore, ISIJ Int. 36 (1996) 1486–1493.
[18] A.J. DeArdo, Int. Mater. Rev. 48 (2003) 371–402.
[19] R. Lagneborg, T. Siwecki, S. Zajac, B. Hutchinson, Scand. J. Metall. 28 (1999) 186–241.
[20] R. Lagneborg, S. Zajac, Metall. Mater. Trans. A 31A (2000) 1–12.
[21] S. Zajac, T. Siwecki, W.B. Hutchinson, R. Lagneborg, ISIJ Int. 38 (1998) 1130–1139.
[22] P. Li, J.A. Todd, Metall. Trans. A 19A (1988) 2139–2151.
[23] F.A. Khalid, D.V. Edmonds, Mater. Sci. Technol. 9 (1993) 384–396.
[24] N.K. Balliger, R.W.K. Honeycombe, Metall. Trans. A 11A (1980) 421–429.
[25] F. Perrard, P. Donnadieu, A. Deschamps, P. Barges, Philos. Mag. 86 (2006) 4271–4284.
[26] R.D.K. Misra, H. Nathani, J.E. Hartmann, F. Siciliano, Mater. Sci. Eng. A 394 (2005) 339–352.
[27] A. Ghosh, B. Mishra, S. Das, S. Chatterjee, Mater. Sci. Eng. A 396 (2005) 320–332.
[28] C.P. Reip, S. Shanmugam, R.D.K. Misra, Mater. Sci. Eng. A 424 (2006) 307–317.
[29] S. Shanmugam, R.D.K. Misra, T. Mannering, D. Panda, S.G. Jansto, Mater. Sci. Eng. A 437 (2006) 436–445.
[30] R.W.K. Honeycombe, Steels Microstructure and Properties, Edward Arnold, London, 1980.
[31] M.J. Balart, C.L. Davis, M. Strangwood, Mater. Sci. Eng. A 284 (2000) 1–13.
[32] M.J. Balart, C.L. Davis, M. Strangwood, Mater. Sci. Eng. A 328 (2002) 48–57.
[33] M.J. Balart, C.L. Davis, M. Strangwood, Scripta Mater. 50 (2004) 371–375.
[34] A. Echeverria, J.M. Rodriguez-Ibabe, Scripta Mater. 50 (2004) 307–312.
[35] D.P. Fairchild, D.G. Howden, W.A.T. Clark, Metall. Mater. Trans. A 31A (2000) 641–652.

Please cite this article in press as: H. Najafi, et al., Mater. Sci. Eng. A (2007), doi:10.1016/j.msea.2007.08.057